Inorganic Chemistry
Article

Inorg. Chem. **2009**, *48*, 7413–7420 **7413**
DOI: 10.1021/ic900980y

Tetranuclear Coordination Assemblies Based on Half-Sandwich Ruthenium(II) Complexes: Noncovalent Binding to DNA and Cytotoxicity

Fátima Linares,[†] Miguel A. Galindo,[‡] Simona Galli,[§] M. Angustias Romero,[†] Jorge A. R. Navarro,*[,†] and Elisa Barea*[,†]

[†]*Departamento de Química Inorgánica, Universidad de Granada, Av. Fuentenueva S/N, 18071 Granada, Spain,* [‡]*School of Chemistry, Newcastle University, Bedson Building, Newcastle Upon Tyne, NE1 7RU, United Kingdom, and* [§]*Dipartimento di Scienze Chimiche e Ambientali, Università dell'Insubria, Via Valleggio 11, 22100 Como, Italy*

Received May 19, 2009

The reaction of $[(cymene)RuCl_2]_2$ with K_2Hoxonate (H_3oxonic=4,6-dihydroxy-2-carboxy-1,3,5-triazine acid) in methanol leads to the formation of the dinuclear half-sandwich ruthenium(II) complex $[(cymene)_2Ru_2(\mu\text{-Hoxonato})Cl_2]$ (**1a**). Removal of the chloride ligands of **1a** by treatment with $AgCF_3SO_3$ yields $[(cymene)_2Ru_2(\mu\text{-Hoxonato})(CF_3SO_3)_2]$ (**1b**), which, upon posterior reaction with *N,N′*-linkers (L=4,4′-bipyridine (4,4′-bpy), 4,7-phenantroline (4,7-phen)), gives rise to the formation of the tetranuclear open boxes $[(cymene)_4Ru_4(\mu\text{-Hoxonato})_2(\mu\text{-}N,N'\text{-L})_2](CF_3SO_3)_4$ (**2a**, L=4,4′-bpy; **2b**, L= 4,7-phen). These systems have been characterized by ^{1}H NMR, UV−vis, and ESI-MS. The single-crystal structures of the dinuclear precursor **1a** and of the clathrate **2b⊂4,7-phen** have been determined. The interaction of these systems with cysteine, mononucleotides, and calf-thymus DNA has been studied by means of ^{1}H NMR, UV−vis, circular dicroism, competitive binding assays, and atomic force microscopy imaging. The results show that the robust tetracationic ruthenium(II) cyclic systems **2a** and **2b** do not give ligand exchange reactions toward biorelevant ligands. Nevertheless, these systems are able to noncovalently bind to DNA, probably at the surface of the major groove, inducing significant conformational changes in this biomolecule. It is also interesting to note that compounds **2a** and **2b**, in spite of only giving supramolecular interactions with biomolecules, exhibit antitumor activity, particularly toward the human ovarian cancer cell line A2780*cis*R, showing acquired resistance to *cisplatin*, with respective 4.6 and 8.3 microM IC_{50} values.

Introduction

The unwanted side effects of the treatment of cancer patients with *cisplatin* and related metallodrugs[1] have prompted the research of alternative systems with a different chemical nature. In this regard, the organometallic half-sandwich ruthenium(II) complexes of the type $[(\eta^6\text{-arene})Ru(YZ)(X)]$, where YZ is, typically, a chelating ligand and X is a halide, are currently the subject of interest as a result of their in vitro and in vivo anticancer activity.[2] Although, like *cisplatin*, these systems have also been shown to give rise to coordinative binding to DNA (through N7 of guanine),[3,4] their biological chemistry is quite different.[4,5] It is also interesting to note the recent report of Therrien and co-workers on the ability of a half-sandwich ruthenium-based coordination cage to encapsulate $[M(acac)_2]$ ($M = Pt^{2+}$, Pd^{2+}) complexes with a synergic enhancement of their antitumor activity.[6] On the other hand, we and others have shown that polynuclear coordination assemblies like iron(II)[7] and ruthenium(II) helicates,[8] as well as Fujita's platinum(II) coordination squares[9] and metallacalixarenes,[10,11]

*To whom correspondence should be addressed. E-mail: ebaream@ugr.es (E.B.), jarn@ugr.es (J.A.R.N.).

(1) *Cisplatin, Chemistry and Biochemistry of A Leading Anti-Cancer Drug*; Lippert, B., Ed.; Wiley-VCH: Weinheim, Germany, 1999.
(2) Aird, R.; Cummings, J.; Ritchie, A.; Muir, M.; Morris, R.; Chen, H.; Sadler, P.; Jodrell, D. *Br. J. Cancer* **2002**, *86*, 1652–1657.
(3) Galindo, M. A.; Quirós, M.; Romero, M. A.; Navarro, J. A. R. *J. Inorg. Biochem.* **2008**, *102*, 1025–1032.
(4) Yan, Y. K.; Melchart, M.; Habtemariam, A.; Sadler, P. J. *Chem. Commun.* **2005**, 4764–4776.
(5) (a) Ang, W. H.; Dyson, P. J. *Eur. J. Inorg. Chem.* **2006**, 4003–4018. (b) Hannon, M. J. *Pure Appl. Chem.* **2007**, *79*, 2243–2261.
(6) Therrien, B.; Süss-Fink, G.; Govindaswamy, P.; Renfrew, A. K.; Dyson, P. J. *Angew. Chem., Int. Ed.* **2008**, *47*, 3773–3776.
(7) (a) Hannon, M. J.; Moreno, V.; Prieto, M. J.; Molderheim, E.; Sletten, E.; Meistermann, I.; Isaac, C. J.; Sanders, K. J.; Rodger, A. *Angew. Chem., Intl. Ed.* **2001**, *40*, 879–884. (b) Hotze, A. C. G.; Hodges, N. J.; Hayden, R. E.; Sanchez-Cano, C.; Paines, C.; Male, N.; Tse, M.-K.; Bunce, C. M.; Chipman, J. K.; Hannon, M. J. *Chem. Biol.* **2008**, *15*, 1258–1267. (c) Hannon, M. J. *Chem. Soc. Rev.* **2007**, *36*, 280–295.
(8) Pascu, G. I.; Hotze, A. C. G.; Sanchez-Cano, C.; Kariuki, B M.; Hannon, M. J. *Angew. Chem., Int. Ed.* **2007**, *46*, 4374–4378.
(9) (a) Mounir, M.; Lorenzo, J.; Ferrer, M.; Prieto, M. J.; Rossell, O.; Aviles, F. X.; Moreno, V. *J. Inorg. Biochem.* **2007**, *101*, 660–666. (b) Kieltyka, R.; Englebienne, P.; Fakhoury, J.; Autexier, C.; Moitessier, N.; Sleiman, H. F. *J. Am. Chem. Soc.* **2008**, *130*, 10040–10041.
(10) Galindo, M. A.; Olea, D.; Romero, M. A.; Hannon, M. J.; Rodger, A.; Gómez, J.; del Castillo, P.; Zamora, F.; Navarro, J. A. R. *Chem.—Eur. J.* **2007**, *13*, 5075–5081.
(11) Galindo, M. A.; Romero, M. A; Navarro, J. A. R. *Inorg. Chim. Acta* **2009**, *362*, 1027–1030.

Published on Web 07/08/2009

Scheme 1. Formation Reaction of the $[(Cymene)_4Ru_4(Hoxonato)_2(N,N'\text{-}L)_2](CF_3SO_3)_4$ (**2a**, L = 4,4′-bpy; **2b**, L = 4,7-phen) Cyclic Assemblies

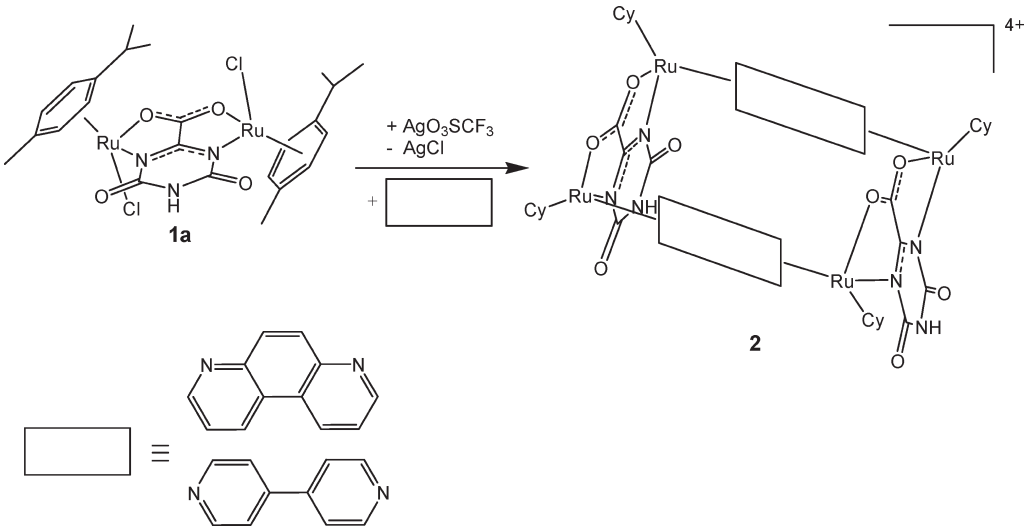

noncovalently bind to DNA with a concomitant biological effect (i.e., antitumor activity, telomerase inhibition). Likewise, Fujita and co-workers have very recently reported the isolation effect exerted by Pt(II) coordination cages, which strongly stabilize the minimal nucleotide duplex formation in highly competitive aqueous solutions.[12]

The above-mentioned results prompted us to study new examples of systems able to give unconventional interactions with biomolecules in order to find new ways to overcome some problems encountered with classical metallodrugs. In this manuscript, we show a strategy to build a series of cationic cyclic polynuclear half-sandwich ruthenium(II) complexes of the $[(cymene)_4Ru_4(\mu\text{-Hoxonato})_2(\mu\text{-}N,N'\text{-L})_2](CF_3SO_3)_4$ kind (**2a**, L = 4,4′-bpy; **2b**, L = 4,7-phen), containing Hoxonato bridges (H_3oxonic = 4,6-dihydroxy-2-carboxy-1,3,5-triazine acid) and N,N'-linkers (4,4′-bipyridine (4,4′-bpy), 4,7-phenanthroline (4,7-phen); Scheme 1). In addition, we have essayed the interaction of these systems with DNA and their citotoxic activity toward human lung and ovarian tumor cell lines. We have chosen the Hoxonato system with the purpose of creating a π-acidic surface able to give specific interactions with nucleotides through anion$-\pi$ interactions[13] and complementary H-bonding interactions.[14]

Experimental Section

Materials. $[(\eta^6\text{-p-Cymene})RuCl_2)]_2$ was prepared according to literature methods.[15] Oxonic acid potassium salt (KH_2oxonate), 4,4′-bipyridine (4,4′-bpy), and 4,7-phenanthroline (4,7-phen) were acquired from commercial sources and used as received.

Synthesis. **[(Cymene)$_2$Ru$_2$Cl$_2$(Hoxonato)] (1a).** $[(\eta^6\text{-p-Cymene})Ru(Cl)_2]_2$ (612 mg, 1.0 mmol) and oxonic acid potassium salt (195 mg, 1 mmol) were suspended in methanol (30 mL). KOH (40 mg, 0.7 mmol) was added to the suspension, and the resulting mixture was refluxed at 70 °C for 6 h to give, upon cooling, an orange precipitate which was filtered off. Crystals suitable for X-ray diffraction were obtained by slow evaporation of a $CHCl_3$ solution (544 mg, 78.1% yield). ^{1}H NMR (400 MHz, DMSO-d_6, 25 °C): δ 1.08 (m, 12H, CH_3-cymene), 2.07 (s, 6H, CH_3-cymene), 2.65 (m, 2H, CH-cymene), 5.58 (d, 2H, aromatic H-cymene), 5.71 (d, 2H, aromatic H-cymene), 5.81 (d, 2H, aromatic H-cymene), 5.92 (d, 2H, aromatic H-cymene), 11.80 (s, 1H, NH-oxonatoH). Elem Anal. Calcd (%) for $C_{24}H_{31}N_3O_4Cl_2Ru_2$: C, 41.26; H, 4.47; N, 6.02. Found: C, 41.06; H, 4.11; N, 6.02.

[(Cymene)$_2$Ru$_2$(CF$_3$SO$_3$)$_2$(Hoxonato)]$_2$ (1b). Solid $Ag(CF_3SO_3)$ (2 mmol, 513 mg) was added to a suspension of $[(cymene)_2Ru_2Cl_2(Hoxonato)]$ (**1a**) (1 mmol, 696 mg) in methanol. The mixture was stirred in the dark at 40 °C for 120 min. Subsequent filtration of AgCl led to isolation of an orange solution which contained the expected compound (795 mg, 82.6% yield). ^{1}H NMR (400 MHz, DMSO-d_6, 25 °C): δ 1.10 (m, 12H, CH_3-cymene), 2.08 (m, 6H, CH_3-cymene), 2.63 (m, 2H, CH-cymene), 6.06 (m, 7H, aromatic H-cymene), 6.45 (m, 1H, aromatic H-cymene), 11.87 (s, 1H, NH-oxonatoH). Elem Anal. Calcd (%) for $C_{26}H_{31}N_3O_{10}S_2F_6Ru_2$: C, 32.53; H, 3.47; N, 4.38; S, 6.68. Found: C, 31.29; H, 3.33; N, 4.25; S, 7.21.

[(Cymene)$_4$Ru$_4$(Hoxonato)$_2$(4,4′-bpy)$_2$](CF$_3$SO$_3$)$_4$(H$_2$O)$_3$ (2a). Solid 4,4′-bipyridine (1 mmol, 156 mg) was added to a solution of compound **1b** (1 mmol in 15 mL of MeOH). The resulting solution was stirred at room temperature for 24 h and then was allowed to stand. After one day, an orange precipitate of **2a** was isolated (670 mg, 60.4% yield). ^{1}H NMR (400 MHz, DMSO-d_6, 25 °C): δ 1.15 (dd, 12H, CH_3-cymene), 1.71 (s, 6H, CH_3-cymene), 2.70 (m, 2H, CH-cymene), 5.90 (d, 4H, aromatic H-cymene), 6.22 (d, 4H, aromatic H-cymene), 7.65 (d, 4H, 4,4′-bpy), 8.06 (d, 4H, 4,4′-bpy), 12.58 (s, 1H, NH-oxonatoH). FTMS (+ESI): m/z 931.05 $[M - 2CF_3SO_3]^{2+}$. Elem Anal. Calcd (%) for $C_{72}H_{80}N_{10}O_{23}S_4F_{12}Ru_4$: C, 39.06; H, 3.64; N, 6.33; S, 5.79. Found: C, 38.60; H, 3.88; N, 6.37; S, 6.27.

[(Cymene)$_4$Ru$_4$(oxonatoH)$_2$(4,7-phen)$_2$](CF$_3$SO$_3$)$_4$(CH$_3$OH) (2b). To a solution of compound **1b** (1 mmol in 15 mL of MeOH) was added solid 4,7-phenanthroline (1 mmol, 180 mg). The mixture was stirred for 24 h to give an orange solid of **2b** (451 mg, 40.8% yield). ^{1}H NMR (400 MHz, DMSO-d_6, 25 °C): δ 1.12 (dd, 6H, CH_3-cymene), 1.28 (dd, 6H, CH_3-cymene), 1.58 (s, 6H, CH-cymene), 2.07, 2.72 (m, 2H, CH-cymene), 5.94 (d, 2H, aromatic H-cymene), 6.19 (d, 2H, aromatic H-cymene), 6.28 (d, 2H, aromatic H-cymene), 6.52 (d, 2H, aromatic H-cymene), 7.55 (s, 2H, 4,7-phen), 7.69 (m, 1H, 4,7-phen), 8.07 (s, 2H, 4,7-phen), 8.32 (s, 2H, 4,7-phen), 8.80 (s, 1H, 4,7-phen), 9.07 (s, 2H, 4,7-phen), 9.18 (d, 1H, 4,7-phen), 12.80 (s, 1H, NH-oxonatoH).

(12) Sawada, T.; Yoshizawa, M.; Sato, S.; Fujita, M. *Nature Chem.* **2009**, *1*, 53–56.
(13) (a) Gamez, P.; Mooibroek, T. J.; Teat, S. J.; Reedijk, J. *Acc. Chem. Res.* **2007**, *40*, 435–444. (b) Schottel, B. L.; Chifotides, H. T; Dunbar, K. R. *Chem. Soc. Rev.* **2008**, *37*, 68–83.
(14) Schlawe, D.; Majdalani, A.; Velcicky, J.; Hessler, E.; Wieder, T.; Prokop, A.; Schmalz, H.-G. *Angew. Chem., Int. Ed.* **2004**, *43*, 1731–1734.
(15) Komiya, S. *Synthesis of Organometallics Compounds*; John Wiley & Sons: New York, 1997; Chapter 8.

FTMS (+ESI): m/z 955.05 $[M - 2CF_3SO_3]^{2+}$. Elem Anal. Calcd (%) for $C_{77}H_{78}N_{10}O_{21}S_4F_{12}Ru_4$: C, 41.29; H, 3.51; N, 6.25; S, 5.73. Found: C, 42.46; H, 3.74; N, 6.58; S, 6.11.

Crystals of **2b⊂4,7-phen** suitable for X-ray diffraction were grown from a MeOH solution of **2b** in the presence of an excess of 4,7-phen.

Characterization and Physical Measurements. The ^{1}H NMR experiments carried out for characterizing compounds **1a**, **1b**, **2a**, and **2b** and for studying the interaction between cyclic systems, nucleotides, and cysteine were performed in D_2O and DMSO-d_6 solutions with 10 mg of the compound and 0.75 mL of the solvent. High-temperature experiments were run in DMSO-d_6 with the aim of studying the conformational flexibility of the cyclic systems. ^{1}H NMR spectra were recorded with a Bruker ARX 400 (400 MHz; Centre of Scientific Instrumentation of the University of Granada). ESI-MS measurements were performed by dissolving the samples in methanol and making measurments on a Waters Micromass LCT Premier mass spectrometer. Elemental (C, H, N) analyses were obtained at a FISONS-CARLO ERBA EA 1008 analyzer at the Centre of Scientific Instrumentation of the University of Granada. Molecular geometries of compounds **2a** and **2b** were optimized with molecular mechanics (MMFF) by using the Spartan'04 program package (Wave Function Inc.).

X-Ray Crystallography. Table 1 summarizes the crystallographic data for **1a** and **2b⊂4,7-phen**. The single-crystal X-ray diffraction data for species **1a** were acquired at room temperature from an orange platelet single crystal of approximate 0.10 × 0.10 × 0.05 mm dimensions, on an Enraf Nonius CAD4 automated diffractometer using graphite-monochromated Mo Kα radiation (λ = 0.71073 Å). The unit cell was determined on the basis of the setting angles of 25 randomly distributed reflections in the $9.5 < \theta < 14.4°$ range. The data collection was performed in the $3.0 < \theta < 25.3°$ range by applying the ω-scan mode [$\Delta\omega = 1.1 + (0.35 \tan\theta)$]. A total of 4678 unique and 3025 observed [$I > 2\sigma(I)$] reflections were collected [R(int) = 0.008, $R(\sigma)$ = 0.085] and used for the structure solution and the structure refinement (against 316 parameters). The data were corrected for absorption[16] and Lorenz-polarization effects. The structure was solved by direct methods[17] and refined by full-matrix least-squares on F^2.[18] All of the non-hydrogen atoms were refined anisotropically. Hydrogen atoms were made riding their parent atoms with an isotropic temperature factor 1.2 times that of their parent atoms.

The single-crystal X-ray diffraction data for species **2b⊂4,7-phen** were acquired at 100 K from an orange prism single crystal of approximate 0.24 × 0.18 × 0.14 mm dimensions, on a Bruker APEX automated diffractometer using graphite-monochromated Mo Kα radiation (λ = 0.71073 Å). The data collection was performed in the $1.14 < \theta < 26.4°$ range by applying the ω-scan mode. A total of 19 586 unique and 18 078 observed [$I > 2\sigma(I)$] reflections were collected [R(int) = 0.056, $R(\sigma)$ = 0.036] and used for the structure solution and the structure refinement (against 1125 parameters). The data were corrected for absorption[19] and Lorenz-polarization effects. The structure was solved by direct methods[17] and refined by full-matrix least-squares on F^2.[18] All of the non-hydrogen atoms were refined anisotropically, except for those of the solvent and of the triflate anions (S excluded). Hydrogen atoms were made riding their parent atoms with an isotropic temperature factor 1.2 times that of their parent atoms. The measured single crystal was twinned (with 0.72:0.28 refined components ratio). A rotational disorder of the CF_3 and SO_3 groups severely affected the triflate anions, an annoying but expected, and well-documented, phenomenon. The disorder determined the presence of non-negligible peaks of electron density nearby the triflate anions. Attempts to reasonably model this disorder were not successful. Nevertheless, it is worth noting that its presence does not affect the structural features of the Ru(II) tetranuclear complex.

Table 1. Crystallographic Data and Refinement Parameters for Species **1a** and **2b⊂4,7-phen**

	1a	**2b⊂4,7-phen**
formula	$C_{24}H_{28}Cl_2N_3O_4Ru_2$	$C_{89}H_{88}F_{12}N_{12}O_{21}Ru_4S_4$
fw (g mol^{-1})	695.5	2422.3
T (K)	298(2)	100(2)
λ (Å)	0.71073	0.71073
cryst syst	monoclinic	orthorhombic
space group	$P2_1/c$	$P2_12_12_1$
a (Å)	12.609(2)	14.1402(5)
b (Å)	12.810(4)	21.9479(6)
c (Å)	16.720(6)	30.7251(9)
α (deg)	90	90
β (deg)	107.35(2)	90
γ (deg)	90	90
V (Å^3)	2578(1)	9535.5(5)
Z	4	4
ρ(calcd) (Mg m^{-3})	1.415	1.687
μ (Mo Kα, mm^{-1})	1792	0.810
F(000)	1388	4888
sample size (mm^3)	0.10 × 0.10 × 0.05	0.24 × 0.18 × 0.14
2θ range (deg)	6.0−50.6	2.28−52.8
hkl range	$-15 \le h \le 14$	$-17 \le h \le 17$
	$-3 \le k \le 15$	$-27 \le k \le 27$
	$-8 \le l \le 20$	$-38 \le l \le 38$
unique, observed reflns	4678, 3025	19586, 18078
R(int), $R(\sigma)$	0.008, 0.085	0.056, 0.036
data, restraints, params	4678, 0, 316	19586, 0, 1102
$\chi(F^2)$[a]	1.044	1.611
$R(F)$, $wR(F^2)$ for $I > 2\sigma(I)$[a]	0.052, 0.087	0.065, 0.193
$R(F)$, $wR(F^2)$ for all reflns[a]	0.103, 0.102	0.071, 0.197
highest peak, deepest hole (e Å^{-3})	0.653, −0.611	4.01, −1.65

[a] $\chi(F^2) = [\sum w(F_o^2 - F_c^2)^2/(n-p)]^{1/2}$, where n is the number of reflections, p is the number of parameters, and $w = 1/[\sigma^2(F_o^2) + (0.019P)^2 + 1.88P]$, with $P = (F_o^2 + 2F_c^2)/3$. $R(F) = \sum||F_o| - |F_c||/\sum|F_o|$ and $wR(F^2) = [\sum w(F_o^2 - F_c^2)^2/\sum wF_o^4]^{1/2}$.

Crystallographic data (excluding structure factors) for species **1a** and **2b⊂4,7-phen** have been deposited with the Cambridge Crystallographic Data Centre as supplementary publication nos. 714114−714115. Copies of the data can be obtained, free of charge, on application to CCDC, 12 Union Road, Cambridge CB2 1EZ, United Kingdom (fax: +44-(0)1223−336033 or e-mail: deposit@ccdc.cam.ac.uk).

DNA Binding Studies. Calf-thymus DNA (ct-DNA) was purchased from Sigma/Aldrich. The ct-DNA was dissolved in water without any further purification and kept frozen until the day of the experiment. The ct-DNA concentration (moles of bases per liter) was determined spectroscopically by using the molar extinction coefficients at the maximum of the long-wavelength absorbance (ct-DNA ε_{258} = 6600 cm^{-1} mol^{-1} dm^3). Concentrations of stock solutions of compounds **1b**, **2a**, and **2b** were determined from accurately weighed samples of these materials. A stock sodium cacodylate buffer (100 mM) was prepared by mixing a 50 mL solution of sodium cacodylate (0.2 M, 4.24 g of $Na(CH_3)_2AsO_2 \cdot 3H_2O$ in 100 mL) with 9.3 mL of hydrochloric acid (0.2 M) and diluting it to a total of 100 mL. Stock solutions of **1b**, **2a**, and **2b** (500 μM) were prepared. All ct-DNA experiments were conducted in a sodium cacodylic buffer (1 mM) and NaCl (20 mM). Spectroscopic titration series

(16) North, A. T. C.; Phillips, D. C.; Mathews, F. S. *Acta Crystallogr.* **1968**, *A24*, 351–359.

(17) SIR97: Altomare, A.; Burla, M. C.; Camalli, M.; Cascarano, G. L.; Giacovazzo, C.; Guagliardi, A.; Moliterni, A. G. G.; Polidori, G.; Spagna, R. *J. Appl. Crystallogr.* **1999**, *32*, 115.

(18) Sheldrick, G. M. *SHELX-97*; University of Göttingen: Göttingen, Germany, 1997.

(19) Sheldrick, G. M. *SADABS*; University of Göttingen: Göttingen, Germany, 1996.

experiments keeping the ct-DNA concentration constant were undertaken by adding the salt, buffer, water, and the cyclic assembly to the ct-DNA. The circular dichroism (CD) spectra were produced by using a Jasco J-715 spectropolarimeter. UV−vis was performed and visualized using a ThermoSpectronic UV300 using 2 mL of an aqueous solution of ct-DNA (150 μM) in NaCl (20 mM) and a sodium cacodylate buffer (1 mM). The previously described solutions were used to register the UV/vis spectra, adding increased quantities of compounds **2a** and **2b** and keeping the ct-DNA concentration constant (ct-DNA/metal complexes' mixing ratios range from 200:1 to 5:1).

Ethidium bromide (EB) displacement by the cyclic assemblies was calculated by measuring the quenching of the EB fluorescence as it leaves the protection of the ct-DNA. A ct-DNA/salts/buffer solution with EB (4:5 ct-DNA/EB, 4:5 mM) was prepared. The emission spectrum was recorded as a function of **1b**, **2a**, and **2b** concentrations using a Variant mod Cary Eclipse Luminescence spectrometer, and the ruthenium complex concentration was slowly increased for ct-DNA/metal-complex ratios from 70:1 to 1:1, keeping the ct-DNA and EB concentrations constant. After each addition, the fluorescence and UV−visible spectra were recorded (parameters: emission, 600 nm; excitation, 540 nm; excitation slit, 10.0 nm; emission slit, 15.0 nm).

Atomic Force Microscopy Imaging (AFM). Adsorption of blank calf-thymus DNA proceeded as follows. Samples were prepared by depositing a drop (10 μL) of a ct-DNA solution (30 μM) containing $MgCl_2$ (4 mM) onto a mica sheet. After adsorption for 1 min at room temperature, the samples were gently rinsed with milli-Q quality water and dried with nitrogen. Adsorption of ct-DNA complexes proceeded as follows, incubation of ct-DNA with **2a** and **2b**: Solutions of ct-DNA (30 μM) containing $MgCl_2$ (4 mM) were incubated at room temperature with **2a** and **2b** (three base pairs/complex) for 1 h. A drop of these solutions (10 μL) was deposited onto a sheet of mica for 1 min. The samples were rinsed and dried as described above. AFM imaging proceeded as follows: AFM imaging was performed in the air by using the tapping mode on a Multimode Nanoscope IIIa (Veeco, Metrology group) and NanoProbe tips (Veeco Inc.). Vibrational noise was reduced with an isolation system (Manfrotto).

Biological Assays. Cytotoxic studies were performed at the Unidad de Evaluación de Actividades Farmacológicas, Instituto de Farmacia Industrial, Facultad de Farmacia, University of Santiago de Compostela, 15782 Santiago de Compostela, Spain. The tumor cell lines A2780 and A2780cisR were cultured at 37 °C in RPMI 1640 medium (Gibco) supplemented with 10% fetal bovine serum and 2 mM L-glutamine in an atmosphere of 95% air and 5% CO_2. Cell death was evaluated by using a system based on the tetrazolium compound 3-(4,5-dimethyl-2-thiazolyl)-2,5-diphenyl-2*H*tetrazolium bromide (MTT), which is reduced by living cells to yield a soluble formazan product that can be detected colorimetrically. Cells were seeded in 96-well sterile plates at a density of 4000 cells/well in 100 μL of medium and were incubated for 24 h. Complexes dissolved in DMSO were added to final concentrations ranging from 0 to 1.1 10^{-4} M at a volume of 100 μL/well. The final concentration of DMSO in the cell culture was maintained in all cases at 1%. Ninety-six hours later, 10 μL of a freshly diluted MTT solution (2.5 mg/mL) was pipetted into each well, and the plate was incubated at 37 °C in a humidified 5% CO_2 atmosphere. After 5 h, the medium was removed, and the obtained formazan product was dissolved in 100 μL of DMSO. The cell viability was evaluated by measurement of the absorbance at 595 nm. IC_{50} values (compound concentration that produces 50% cell growth inhibition) were calculated from curves constructed by plotting cell survival (%) versus drug concentration (μM). All experiments were made in triplicate.

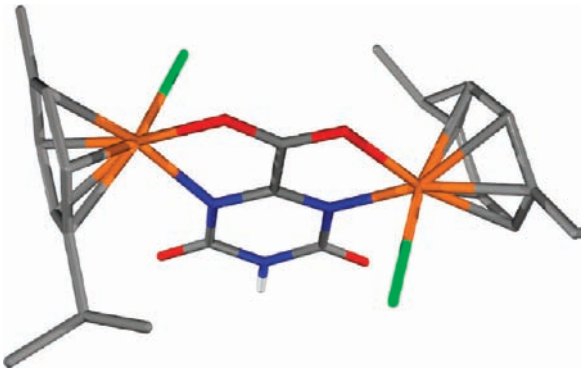

Figure 1. Crystal structure of $[(cymene)_2Ru_2(\mu\text{-Hoxonato})Cl_2]$ (**1a**). Color scheme: C (gray), N (blue), O (red), Ru (orange), Cl (green). H atoms with the exception of the NH moiety have been omitted for the sake of clarity.

Results and Discussion

Formation and Characterization of the Cyclic Assemblies. Reaction of $[(cymene)RuCl_2]_2$ with K_2Hoxonate in a methanolic solution leads to the formation of the dinuclear half-sandwich ruthenium(II) complex $[(cymene)_2Ru_2(\mu\text{-Hoxonato})Cl_2]$ (**1a**). Complex **1a** has been structurally characterized by single-crystal X-ray diffraction. Complex **1a** crystallizes in the monoclinic space group $P2_1/c$. Its asymmetric unit consists of two Ru(II) and two chloride ions, one Hoxonato, and two cymene moieties, all in general positions. The Hoxonato ligands act in a N,O,N',O'-exotetradentate bridging mode, connecting two Ru(II) ions, 5.6 Å apart, within dinuclear $[(cymene)_2Ru_2(\mu\text{-Hoxonato})Cl_2]$ complexes (Figure 1). The coordination sphere of each metal ion is completed by one chloride anion and one η^6-cymene ligand, the chloride ions of the dimer adopting a trans disposition with respect to the mean plane formed by the two Ru(II) ions and the Hoxonato moiety. Intermolecular nonbonding interactions of the Cl···N kind are present between one of the two chloride anions of the complex and the H(N) hydrogen atom on the Hoxonato ring of an adjacent complex, this imparting further stability to the whole crystal structure.

Removal of the chloride ligands of **1a** by treatment with $AgCF_3SO_3$ leads to the formation of $[(cymene)_2Ru_2(\mu\text{-Hoxonato})(CF_3SO_3)_2]$ (**1b**), which, upon posterior reaction with the N,N'-linkers 4,4′-bpy and 4,7-phen, yields the tetranuclear cage complexes $[(cymene)_4Ru_4(Hoxonato)_2(N,N'\text{-L})_2](CF_3SO_3)_4$ (**2a**, L = 4,4′-bpy; **2b**, L = 4,7-phen; Scheme 1). These systems have been studied by ^{1}H NMR and ESI-MS, and their structures have been modeled by molecular force field modeling (Figure 2). The ESI-MS spectra are unequivocally indicative of the formation of the tetranuclear **2a** and **2b** species. It is of note that the $[M - 2CF_3SO_3]^{2+}$ peaks correspond in both cases to the most intense ones in the mass spectra. This feature should be taken as a proof of their high stability. Indeed, ^{1}H NMR spectra for these species in both DMSO-d_6 and D_2O remain unaltered for weeks, which agrees with the robustness of these systems in both solvents. It is of note that, in the case of **2b**, the ^{1}H NMR experiments indicate the presence of two species, which can be attributed to the coexistence of **2b** in its cone and 1,3-alternate conformations, as confirmed by

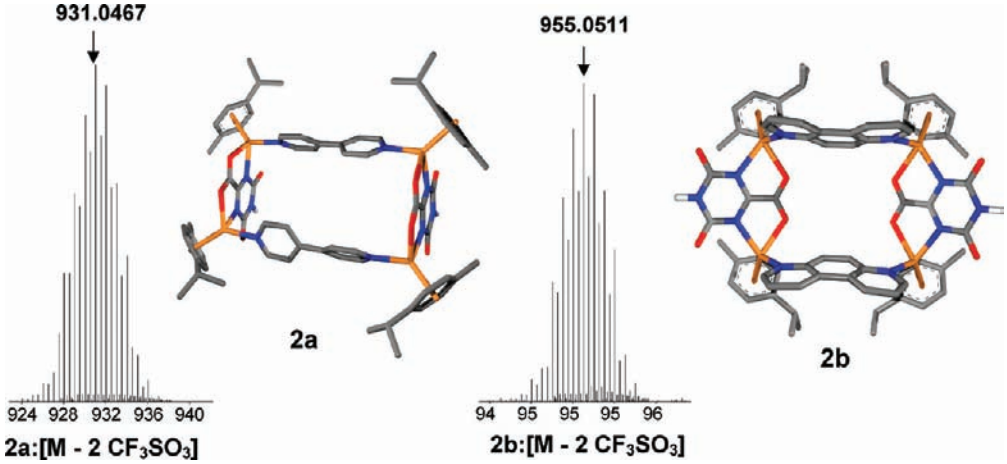

Figure 2. ESI-MS spectrum and molecular force field model of $[(cymene)_4Ru_4(Hoxonato)_2(4,4'\text{-bpy})_2]^{4+}$ (**2a**) and $[(cymene)_4Ru_4(Hoxonato)_2(4,7\text{-phen})_2]^{4+}$ (**2b**).

variable-temperature ^{1}H NMR measurements, which shows the stabilization of the 1,3-alternate conformer at high temperatures.

The X-ray crystal structure investigation on **2b⊂4,7-phen** shows that this species crystallizes in the orthorhombic $P2_12_12_1$ space group, and it is composed of rectangular tetranuclear $[Ru_4(cymene)_4(Hoxonato)_2(4,7\text{-phen})_2]^{4+}$ cationic open boxes (Figure 3), in which the Hoxonato and 4,7-phen ligands show, respectively, *N*,*O*,*N*′,*O*′-exotetradentate and N^4,N^7-exobidentate coordination modes, bridging Ru(II) centers 5.6 and 7.9 Å apart. The open boxes adopt the cone conformation, thereby creating a vaselike cavity suitable for molecular recognition processes. Indeed, the wider entrance of the cone hosts one noncoordinated 4,7-phen molecule, whose shortest atom−atom contacts with the Hoxonato and 4,7-phen cavity walls are, respectively, 3.0 and 3.2 Å. One methanol molecule is placed about the opposite entrance of the cone, while two triflate anions are located nearby. The cohesiveness of the structure is granted also by hydrogen-bond interactions of the (N)H···O type (N···O 2.75, 2.76 Å) involving the nonbonded nitrogen and oxygen atoms of two Hoxonato ligands belonging to distinct, nearby complexes. On the whole, each tetramer is hydrogen-bonded to two adjacent ones, this creating 1-D zigzag strands running approximately along [001]. Weaker hydrogen bonds of the (O)H···O kind (O···O 3.02 Å) are present between the hydroxyl groups of the solvent molecules and the oxygen atoms of nearby triflate anions.

Reactivity and Molecular Recognition Properties of the Ru(II) Assemblies toward Biorelevant Species. The reactivity of $[(cymene)_2Ru_2(Hoxonato)Cl_2]$ (**1a**) toward mononucleotides was studied in both DMSO and aqueous solution by ^{1}H NMR at room temperature and at pH 7.0. The results show that the chloride ligands do not exchange either with the solvent or with the mononucleotides. The addition of a nucleotide in deuterated DMSO is responsible for the widening and shifting of the amine proton resonance of the triazine moiety, which should be indicative of the formation of H-bonding interactions between the Hoxonato moiety and the purine residues of the mononucleotides in low polar solvents like DMSO. In contrast to **1a**, $[(cymene)_2Ru_2(Hoxonato)(CF_3SO_3)_2]$ (**1b**) readily reacts in aqueous solution with guanosine monophosphate and adenosine monophosphate to give the corresponding $[(cymene)_2Ru_2(Hoxonato)(nucleotide)_2]$ adducts.

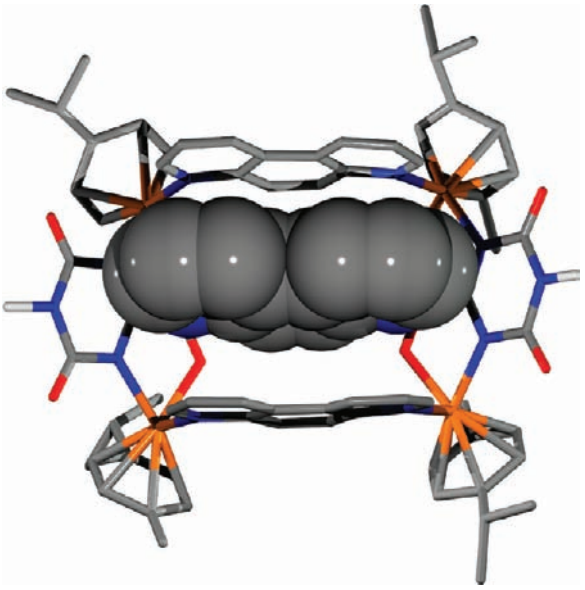

Figure 3. Crystal structure of the supramolecular assembly $[(cymene)_4Ru_4(Hoxonato)_2(4,7\text{-phen})_2⊂4,7\text{-phen}]^{4+}$ (**2b⊂4,7-phen**). Color scheme: C (gray), N (blue), O (red), Ru (orange). H atoms with the exception of the NH moiety have been omitted for the sake of clarity.

The suitability of compounds **2a** and **2b** to act as receptors of mononucleotides has been essayed as a preliminary model of their noncovalent interaction with DNA. In this regard, the presence of the extended aromatic 4,7-phen ligands and the H-bonding features of the Hoxonate moieties suit these systems for giving stacking and complementary H-bonding interactions with nucleobases.

The results show that the addition of a mononucleotide (AMP, GMP) to an aqueous solution of **2a** and **2b** is only responsible for a slight upfield shift of the ^{1}H NMR signals, with no observation of ligand exchange processes. The latter observation is a further proof of the stability of these systems in aqueous solution. Determination of the association constants for the interaction of **2a** or **2b** with

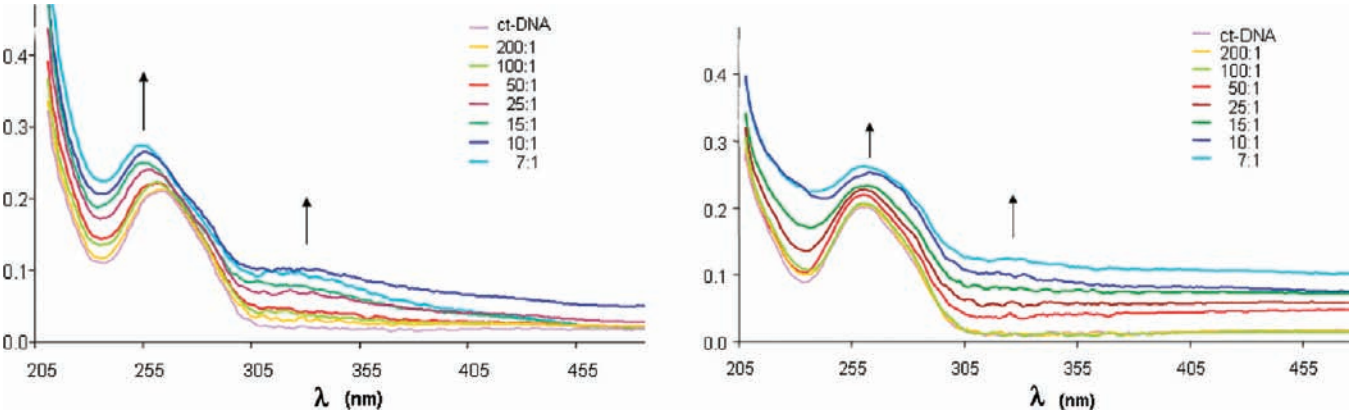

Figure 4. Effect of addition of the coordination assemblies $[(cymene)_4Ru_4(Hoxonato)_2(4,4'\text{-bpy})_2](CF_3SO_3)_4$ (**2a**, left) and $[(cymene)_4Ru_4(Hoxonato)_2(4,7\text{-phen})_2](CF_3SO_3)_4$ (**2b**, right) to a solution of ct-DNA (34 μM) on the UV−vis spectra in a 200:1 to 7:1 ratio. Subtraction of the coordination assemblies' spectra has been made.

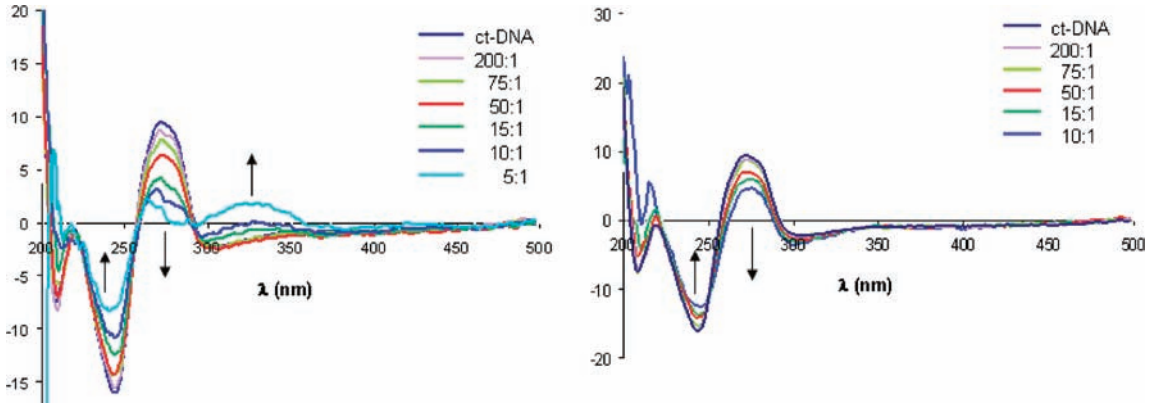

Figure 5. CD spectra of the titration of ct-DNA (300 μM) with $[(cymene)_4Ru_4(Hoxonato)_2(4,4'\text{-bpy})_2](CF_3SO_3)_4$ (**2a**) and $[(cymene)_4Ru_4(Hoxonato)_2(4,7\text{-phen})_2](CF_3SO_3)_4$ (**2b**) in a 200:1 to 5:1 ratio.

mononucleotides in aqueous solution was carried out by means of ^{1}H NMR at pH 7.0.[20] The very low values, $K_{ass} < 4\ M^{-1}$, indicate that the mononucleotides are not incorporated inside the cavity of the receptors but probably interact with their external surface through H-bonding, $\pi-\pi$, anion$-\pi$, and electrostatic interactions. It is also important to mention that these systems also do not react in aqueous solution with S-donor ligands. Indeed, ^{1}H NMR studies show that the incubation of **2a** with 4 equiv of cysteine, over 2 h at 37 °C at pH 7.4, is not responsible for ligand exchange processes. This result suggests that S-donor atoms from other biomolecules (i.e., glutathione, proteins) should not significantly interfere.

DNA Binding Assays. UV−visible absorbance (UV−vis), CD, and EB competitive binding assays were performed in order to assess the capability of these systems to noncovalently bind to DNA. The results indicate that both **2a** and **2b** do efficiently interact with ct-DNA. The UV−vis spectra show an increase in intensity of the characteristic DNA absorption band (λ = 260 nm) upon complex addition (Figure 4). Conversely, the CD spectra (Figure 5) show a significant decrease of the signal ellipticity as a consequence of the same interaction, particularly in the case of the interaction of **2a** with DNA. These results might be indicative of conformational changes in the double strand of DNA as consequence of a supramolecular interaction between the cyclic systems and DNA.[10] In addition, we observe, in the case of the interaction of **2a** with DNA, a complex induced band (λ = 325 nm), which should be taken as further evidence of the interaction of these systems with DNA. In contrast, **1b** is only responsible for a slight diminution of the characteristic DNA absorption band despite its capability to covalently bind to DNA. AFM imaging experiments on the interaction of **2a** and **2b** with DNA also suggest that the interaction of these systems induces significant changes in the shape of the DNA strands, namely, stiffening along with strand aggregation (cross-links; Figure 6). This type of behavior is in contrast with the DNA coiling induced by Hannon's metallocylinder major groove binders[8] but can be related to the conformational changes induced by platinum(II) metallacalixarenes.[10] Taking into account charge, size, and shape considerations, **2a** and **2b** should also fit into the DNA major groove inducing a concomitant distortion in the DNA structure.[21] Moreover, competitive binding assays show a slight diminution in the fluorescence of EB upon complex addition (see the Supporting Information).

(20) Galindo, M. A; Galli, S.; Navarro, J. A. R; Romero, M. A. *Dalton Trans.* **2004**, 2780–2785.

(21) Approximate dimensions for **2a** and **2b** are 2 nm × 1.5 nm × 0.7 and 1.5 nm × 1.5 nm × 0.8 nm, respectively.

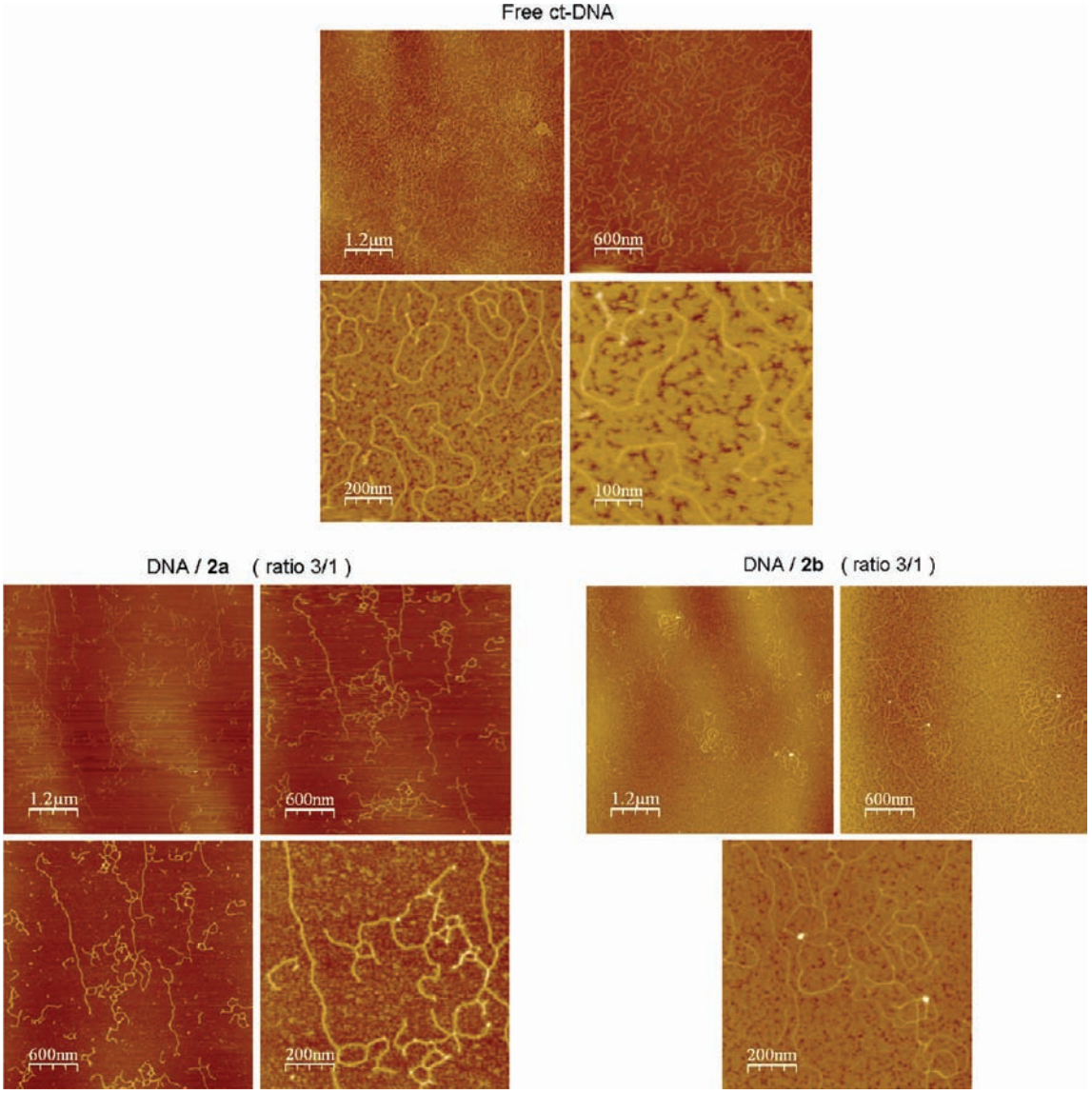

Figure 6. AFM images of free ct-DNA (top) and ct-DNA complexes (ct-DNA−**2a** (left down) and ct-DNA−**2b** (right down)) at a 3:1 DNA base pairs/complex ratio.

This could be related to the displacement of the EB slotted in the DNA major groove in presence of these complexes.

Cytotoxicity Studies. To explore the potential biological effects of the interaction of these systems with biomolecules, we have evaluated their cytotoxicity on human lung NCI-H460, human ovarian A2780, and A2780cisR cancer cell lines. IC_{50} data are reported in Table 2. These systems are not active toward the lung carcinoma NCI-H460 cell line. In the case of the ovarian A2780 cancer cells, it is interesting to observe that, while compound **1a** is not active, compounds **1b**, **2a**, and **2b** show cytotoxic activity against this cell line, although the activities are 20−30 times lower than those exhibited by *cisplatin*. It is of note that the activity of **1b**, **2a**, and **2b** systems toward the A2780cisR cancer cell line with acquired resistance to *cisplatin* is significantly higher, which gives rise to unusually low resistance factors (RF) values.[22] The lack of cytotoxic activity of **1a** was expected in view of its inertness to exchange processes (see above); by contrast, the activity of compounds **2a** and **2b** toward the A2780 cancer cell line is quite striking in view of the noncovalent nature of their interaction with DNA. Moreover, their high activity toward the *cisplatin*-resistant A2780cisR cancer cell line and the very low

Table 2. IC_{50}[a] Values (in μM) in Lung NCI-H460, Ovarian A2780, and *Cisplatin*-Resistant A2780*cis*R Cancer Cell Lines and Resistance Factor RF (IC_{50} *Cisplatin*-Resistant/IC_{50} *Cisplatin*-Sensitive)

compound	NCI-H460	A2780	A2780*cis*R	RF
1a	> 100 μM	> 100 μM	> 100 μM	
1b		20	2.4	0.12
2a	> 100 μM	19	4.6	0.24
2b	> 100 μM	15	8.3	0.55
cisplatin	5.7	0.66	3.7	5.61

[a] IC_{50}: drug concentration necessary for 50% inhibition of cell viability.

(22) Ruiz, J.; Lorenzo, J.; Vicente, C.; López, G.; López de Luzuriaga, J. M.; Monge, M.; Avilés, F. X.; Bautista, D.; Moreno, V.; Laguna, A. *Inorg. Chem.* **2008**, *47*, 6990–7001.

RFs might indicate efficient circumvection of *cisplatin* resistance.[23] On the other hand, the poor activity of these systems toward the lung NCI-H460 cell line might be indicative of a low toxicity of these systems. These features might be taken as a proof of a differentiated mechanism of action of **2a** and **2b** with respect to classical metallodrugs. In this regard, it should be noted that ruthenium metallodrugs, which are currently in clinical trials (NAMI-A and KP1019), like *cisplatin*, possess chloride ligands that can be exchanged in order to bind to biomolecules. It is therefore of high interest to find systems with alternative mechanisms of action. Noncovalent binding of metallodrugs to DNA is an attractive approach; however, most of the effort has been focused on intercalators, with a few exceptions being Hannon's major groove binders of the metallocyclinder type[7,8] and our recent report on platinum(II) metallacalixarenes.[10,11]

Conclusions

We have prepared a series of robust organometallic/coordination Ru(II) cyclic assemblies which do not give ligand exchange reactions either with N-donor biorelevant ligands (nucleobases) or with S-donor biorelevant ligands (cysteine) in aqueous solutions. Nevertheless, these systems are able to interact noncovalently with DNA, inducing significant conformational changes in this biomolecule. These results also imply that different supramolecular drug designs might be used to induce different DNA structural effects. Moreover, the cytotoxic activity toward *cisplatin*-resistant cancer cells suggests that metal coordination assemblies able to bind noncovalently to biomolecules may be a very promising field of research, which may circumvent the heavy metal accumulation problems of platinum and related metallodrugs. It should also be highlighted that the inactivity of these systems toward lung carcinoma NCI-H460 cell lines might be indicative that these kinds of systems are not highly citotoxic and might be selective toward specific cell lines.

Work is in progress in order to systematically control the shape and size of these kinds of assemblies and to study if there is a DNA binding sequence specificity.

Acknowledgment. Funding from the Spanish Ministerio de Educación y Ciencia (CTQ2005-00329/BQU), Junta de Andalucía, Universidad de Granada (Contrato de Incorporación de Doctores (EB)), the Marie Curie program (MAG), and COST-D39 Action are acknowledged.

Supporting Information Available: ^{1}H NMR, UV−vis, CD, and fluorescence spectra. This material is available free of charge via the Internet at http://pubs.acs.org.

(23) Ruiz, J.; Rodríguez, V.; Cutillas, N.; López, G.; Bautista, D. *Inorg. Chem.* **2008**, *47*, 10025–10036.